Computers and Concrete, Vol. 1, No. 1 (2004) 99-113
DOI: http://dx.doi.org/10.12989/cac.2004.1.1.099

Performance of structural-concrete members under sequential loading and exhibiting points of inflection

I. Jelić†

Arup, 155 Avenue of the Americas, New York 10013, USA

M.N. Pavlović‡

Department of Civil and Environmental Engineering, Imperial College, London SW7 2AZ, UK

M.D. Kotsovos‡

Department of Civil Engineering, National Technical University of Athens, Zographou, Athens 15780, Greece

(Received June 10, 2003, Accepted October 9, 2003)

Abstract. The article reports data on, and numerical modelling of, beams exhibiting points of inflection and subjected to sequential loading. Both tests and analysis point to inadequacies in current codes of practice. An alternative design methodology, which is strongly associated with the notion that contraflexure points should be designed as "internal supports", is shown to produce superior performance even though it requires significantly less secondary reinforcement than that advocated by codes.

Keywords: structural concrete; nonlinear finite-element modelling; points of inflection; sequential loading; codes of practice.

1. Introduction

Most available experimental data used for calibrating numerical models for structural concrete are based on tests carried out on statically-determinate (and, usually, simply-supported) beam elements. Furthermore, the loading employed in such tests is almost invariably monotonic. In practice, however, actual structures are multi-element systems of a (sometimes highly) statically-indeterminate nature; and, in addition, sequential loading conditions often need to be taken into account besides the "neater" (especially in limit-state collapse analysis) monotonic (and, in the case of multi-loads, proportional) loading assumption.

What the above simple laboratory tests rarely provide are points of inflection, in sharp contrast to real structures under practical loading conditions. In a recent article (Kotsovos and Pavlović 2001),

† Ph.D.
‡ Professor

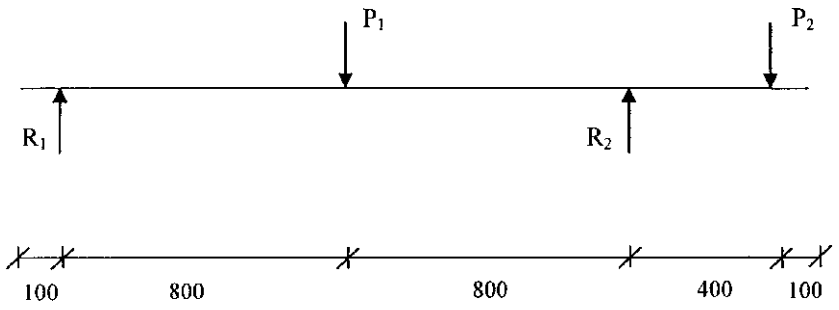

Proportional loading : $P_1=3P_2$

Sequential loading : $P_1=90kN$; P_2=loaded to failure

Fig. 1 Loading arrangement

it was reported that many earthquake failures occur precisely in regions of the structure associated with contraflexure points, suggesting possible design weaknesses in current codes of practice, where no special provision is made for these regions. In order to investigate and address this anomaly, an experimental programme was carried out on structural elements exhibiting points of inflection under both proportional and sequential loadings (Jelić 2002, Jelić, *et al.* 2003). Thus, simply-supported beams with overhangs (shown in Fig. 1) were tested: these beams were designed with a range of different transverse-reinforcement arrangements (as regards both spacing of the stirrups and their cross-sectional areas). Such designs consisted of those adhering to both current code provisions (namely the European codes (EC2 1991, EC8 1991) and the Greek code (GEC 2000)) and the methodology following the compressive-force path (henceforth CFP) concept expounded by Kotsovos and Pavlović (1999).

It is interesting that, contrary to code tenets, it was found that an increase in beam transverse reinforcement does not necessarily equate to an increase in shear capacity or improved ductility in reinforced-concrete (RC) members. On the contrary, the ductility of the beams investigated increased by increasing the spacing of the links and by decreasing their cross-sectional area. In fact, the most overdesigned members (i.e., those designed to EC2 and EC8) sometimes even failed to achieve the required flexural capacity when subjected to sequential loading. The aim of this article is to summarize these results for sequential-loading conditions in terms of both the experimental data and the nonlinear finite-element analysis (NLFEA) that complemented the laboratory work.

2. Specimen details

All beams tested were simply supported with a span of 1600 mm and overhang of 400 mm. Their total lengths were 2200 mm, with a rectangular cross-section of 230 mm(depth)×100 mm(width) (this depth includes a 30 mm distance from the centroid of the bars to the outside face of the beam, for both top and bottom). The loading arrangement, for both proportional and sequential loading, is shown in Fig. 1.

The beams were under-reinforced using two 16 mm diameter high-yield deformed bars;

Table 1 Predicted and experimental bending-moment capacities (kNm/m), and their recorded ductility factors, for the beams tested

Design	Beam reference	Load type	Predicted BM capacity (1)	Experimental BM capacity	(2)/(1) ratio	Ductility factor
EC2 and EC8	HDCB3	Sequential	43.65	45.07	1.03	2.5
	HDCB4	Sequential	43.65	42.60	0.98	2
	MDCB3	Sequential	43.52	41.54	0.95	1.45
	MDCB4	Sequential	43.52	42.56	0.98	2.2
	LDCB3	Sequential	43.58	36.64	0.84	1.45
	LDCB4	Sequential	43.58	38.46	0.88	1.7
GEC	G21	Sequential	39.12	45.93	1.17	5.6
	G22	Sequential	39.12	44.31	1.13	5.6
CFP	B1	Sequential	39.35	43.32	1.10	5.3
	B2	Sequential	39.35	43.62	1.11	6.3
	B3*	Sequential	39.35	44.40	1.13	8.1
	B4*	Sequential	39.35	44.80	1.14	9.6

*denotes additional confinement reinforcement in the compressive region

longitudinal compression reinforcement was also provided, as required by the various codes, since it contributes to ductility (and, in some instances, also to the flexural capacity of the member): the longitudinal reinforcement (16 mm bars) was adopted throughout the whole beam, at both top and bottom so as to cater for the hogging bending moment due to the overhang. The transverse reinforcement provided was in the form of 8 mm plain mild-steel bars. The average test values of yield and ultimate stresses were, respectively, 536 MPa and 626 MPa (16 mm bars) and 368 MPa and 480 MPa (8 mm bars).

The average concrete strength for all beam types was around 30 MPa and the same mix was used throughout. Actual concrete strength was determined by crush tests on cubes and cylinders performed 28 days after casting, with the corresponding beam specimens (listed in Table 1) being tested on the same day: these actual (cylinder) strengths were recorded as 30 MPa (HDCB specimens), 28 MPa (MDCB specimens), 34.25 MPa (G specimens) and 31.40 MPa (B specimens). The effective depth was 200 mm for all twelve beams, while the concrete cover (to both tension and compression reinforcement) was 14 mm except for the four specimens designed to the CFP metodology for which this cover was 16 mm.

Further details on the specimens and their production are reported by Jelić (2002). Information on the test rig, instrumentation, loading and deflection measurement is also contained there.

3. Experimental programme and test results

All beams were tested in the same manner, with the loading arrangement as shown in Fig. 1. Such a simply-supported beam with overhang is, on the one hand, relatively easy to test, while, on the other hand, it provides a point of contraflexure in the main span close to the overhang support and, thus, constitutes a more realistic representation of continuous beams and frame-like structures found

in RC buildings. Hence, the experimental set-up can yield data beyond that on which most other laboratory results are based, namely simply-supported beam tests.

The loading adopted also goes beyond the constraints of most experiments of this type. For, in addition to proportional loading (P1=3P2 in Fig. 1), sequential loading, too, is investigated (by first applying a constant load P1=90 kN at the middle of the main span, and then increasing the other point load P2 at the overhang from zero to failure - see Fig. 1). It is this sequential loading which forms the subject of the present article.

Three types of beam designs were carried out and compared: namely, design to the EC2 and EC8, design to the GEC and, finally, design to the CFP. The nominal beam characteristics as regards dimensions, longitudinal reinforcement and concrete strength were common to all specimens, and hence the various designs differed only in the quantity of transverse reinforcement required by the shear provisions of the relevant code (in the case of the CFP design, the location, as well as the amount of the reinforcement, differed).

The first set of beams was designed in accordance with EC2 and EC8. The beams' flexural capacities were calculated using the method outlined in the EC2 which, essentially, is identical to the one adopted by the British code (BS8110 1985). Now, depending on the location of construction, seismic history and ductility required, EC8 classifies RC beams into three categories: high-ductility class beams (HDCB), medium-ductility class beams (MDCB) and low-ductility class beams (LDCB). The difference between these three types of beams is in the percentage of the concrete shear resistance assumed to contribute to the ultimate shear resistance of the section. Thus, for HDCB no contribution from the concrete shear resistance is assumed, while for MDCB and LDCB, the percentage rises to 40% and 100% respectively.

Shear reinforcement was calculated using the EC2 provisions (again, similar to the ones adopted by BS8110) except in the so-called "critical regions". EC8 defines critical regions as locations where shear has a critical value and identifies them with locations of (a) point loads, (b) supports, (c) bending-moment change (which is usually associated with high shear forces). The length of the critical region depends on the ductility class of the beam and takes on the values $2h$ (HDCB), $1.5h$ (MDCB) and h (LDCB) as appropriate, where h is the overall depth of the section. The spacing of the shear reinforcement (s_v) in critical regions (for beams of all ductility classes) is set to a maximum of $s_v=h/4$. In the remainder of the beam, EC2 provisions apply, setting the maximum spacing of the shear reinforcement as $s_v=0.6d$, where d is the effective depth. Full design calculations for HDCB, MDCB and LDCB are given by Jelić (2002) (Appendices A, B and C respectively). For each class of beam, two specimens were tested for each loading condition in order to check repeatability of results: thus, each pair of beams is defined by suffixes 3 and 4 which refer to sequential loading.

The second series of beams were designed in accordance with the GEC. Its provisions are essentially the same as those of its EC2 and EC8 counterparts, except that in the GEC the length of the critical region is taken as $2h$ (as for the HDCB) and, more notably, maximum spacing of stirrups in the critical region is limited to $s_v=h/3$ (c.f. $h/4$ in EC8); nor does the GEC distinguish between beams of different classes, unlike EC8. In the remainder of the beam, $s_v=0.6d$ (as for EC2). Flexural capacity of beams is calculated from first principles, as for EC2 and EC8. The GEC always assumes full contribution to shear capacity from the uncracked portion of the beam (as for the LDCB in EC8). The design calculations for the beams designed to the GEC are described by Jelić (2002) (Appendix D). Once again, two beams were tested for each loading condition so as to ensure repeatability of results (G21 and G22 denote these specimens subjected to sequential loading).

Finally, the third set of experiments was conducted on beams designed to the CFP method. Full design details are contained in Appendix E of the thesis by Jelić (2002), while the general design methodology can be found in the book by Kotsovos and Pavlović (1999). The latter differs from that of current codes of practice in that, instead of following the concept of a "critical section" (which stems from elastic design guidelines and yet is also applied to ultimate-strength design), skeletal RC structures are designed as a set of "beam-arches" connected at points of inflection by "internal supports" in the form of stirrups: elsewhere in the beams, transverse reinforcement is only required in certain regions of beams with behaviour II or III, but not I or IV (types I to IV cover all beam types - see Kotsovos and Pavlović 1999), with nominal transverse reinforcement (capable of sustaining tensile stresses of the order of 0.5 MPa) throughout the remainder of the span; in addition, allowance is also made for the possibility of bond failure. Altogether, four beams were tested for different design conditions (as before, two nominally identical specimens were employed for result repeatability): sequential loading (B1 and B2); sequential loading but with additional confinement reinforcement in the compression region (B3 and B4).

The experimental results are summarized in Table 1. This contains the bending-moment capacities (both predicted and actually achieved), as well as the measured ductility factors.

4. Numerical modelling

4.1. Background

The beams investigated were analysed by three-dimensional (3D) NLFEA. The FE structural-concrete model used for this purpose is fully described elsewhere (Kotsovos and Pavlović 1995, Kotsovos and Spiliopoulos 1998a, b) and, therefore, only its most important features will be briefly outlined in what follows. It uses a linear FE package called FINEL (Hitchings 1980) within an iterative procedure based on the Newton-Raphson method. The finite elements chosen are the 27-node Lagrangian brick element for concrete modelling, and the matching 3-node parabolic element, with axial stiffness only, for reinforcing bars. The main feature of the model is its heavy dependence on a realistic description of the concrete behaviour at a material level, which sharply contrasts with material descriptions adopted in other FE structural-concrete models (especially as concrete approaches failure).

Unlike most FE models used to date for the analysis of concrete structures, the model employed for the present work incorporates a brittle constitutive model of concrete behaviour. The use of such a constitutive model is compatible with valid experimental information, which demonstrated that the strain-softening material characteristics widely considered to describe the post-peak stress behaviour of concrete reflect the interaction between specimen and testing device (Kotsovos 1982, 1983, Van Mier 1986, Van Mier, *et al.* 1997). Furthermore, it has also been established by experiment that the strains measured in the compressive zone of an RC beam - currently associated with strain-softening characteristics - do, in fact, correspond to triaxial states of stress that lie inside the space enclosed by the failure surface describing the peak-stress conditions (Kotsovos 1982, 1983).

The above constitutive model, which essentially describes the behaviour of "uncracked" concrete, is complemented with an analytical description of the cracking process. These processes involve both the formation and the closure of cracks, the effect of which is considered to be smeared over the whole region corresponding to a "Gauss point". When the calculated values of the principal stresses at a Gauss point define a point in stress space outside the failure surface, a crack is considered to

form on the plane of the maximum and intermediate principal stresses (with the compressive stress being taken as positive) and to open in the orthogonal directional (i.e., the direction of minimum principal stress). Crack formation leads both to loss of load-carrying capacity in the direction orthogonal to the crack plane and to loss of resistance to shearing movement of the crack surfaces in the direction of the maximum principal compressive stress. These two effects are allowed for in the analysis by setting to zero the modulus of elasticity orthogonal to the crack plane and by assigning a small value to the shear modulus on the plane of the maximum and minimum principal stresses. (A small value, rather than zero, is assigned to the shear modulus in order to avoid numerical difficulties.) During subsequent load steps, a compressive strain orthogonal to the crack plane is considered indicative of crack closure, which is described by restoring the material to its "uncracked" state.

The constitutive model used for describing the deformational behaviour of the steel reinforcement in either tension or compression follows current code recommendations on the bilinear characteristic under monotonic loading, so that the stress-strain curve is fully defined by using the values of the yield stress and the ultimate strength together with the values of the corresponding strains, with the yield strain taken as the ratio of the yield stress to the elastic modulus of elasticity. During unloading, the stress-strain behaviour is fully defined by the modulus of elasticity up to the (reversed) yield stress, beyond which it is defined by the post-yield slope of the monotonic stress-strain curve. On the other hand, during reloading the stress behaviour is fully described by the modulus of elasticity under a stress smaller than that previously applied, while for stresses larger than previously applied it is described by the "monotonic" stress-strain curve.

Finally, the assumption of perfect bond is considered to provide an adequate description of the interaction between steel and concrete. This is compatible with the smeared-crack approach adopted for the analytical description of the cracking processes of concrete, as well as the fact that the tensile strength of concrete is smaller than that of the strength of the bond between the two materials.

The nonlinear strategy developed for the nonlinear analysis is based on a version of the well-known incremental Newton-Raphson iterative technique fully described elsewhere (Kotsovos and Pavlović 1995, Zienkiewicz 1977). Allowing the state of loading or unloading to change and crack formation or closure to occur at every iteration causes early divergent analyses due to the build-up of large residual forces and the rapid propagation of spurious mechanisms. In an attempt to prevent early divergence and achieve numerical stability, the iterative procedure has been divided into three stages. The first stage comprises only one iteration within which the structure stiffness matrix K is updated using the initial material properties for the element constitutive matrix D and the state of loading or unloading is established at every Gauss point without allowing the formation or closure of the cracks. Once it is established whether a Gauss point is in a state of loading or unloading, this state remains unchanged to the end of the iterative procedure of the load step. The second stage uses the pure Newton-Raphson method and allows only crack closure (one crack closure per iteration), with the iterations continuing until all cracks due for closure do, in fact, close. Finally, within the third stage, the iterative procedure uses a modified version of the Newton-Raphson method, in that the D-matrices are updated as soon as nonlinearities occur and allows only crack formation to occur, with the iterations continuing until either a convergent solution is obtained or the run stops due to ill-conditioning.

4.2. Mesh discretization adopted

The concrete is modelled by means of 27-node Lagrangian elements. Longitudinal and transverse

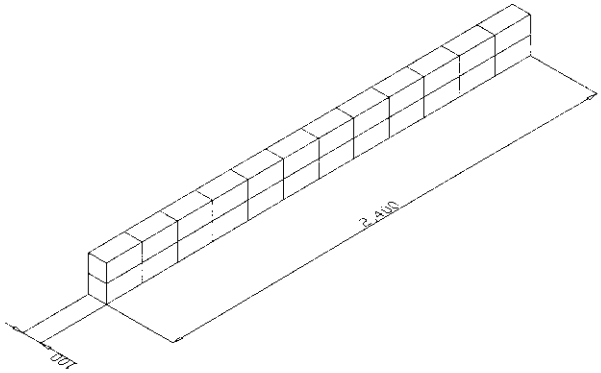

(a)

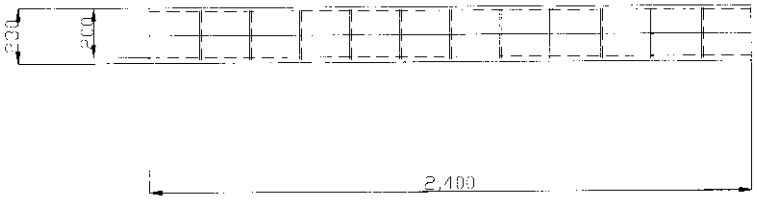

(b)

Fig. 2 Mesh discretization used in the NLFEA: (a) 24 Lagrangian elements for concrete (all beams); (b) line elements for the steel reinforcement (shown by the dotted lines) for beams HDCB3 and HDCB4

reinforcement is represented by 3-noded line elements of appropriate cross-sectional areas possessing axial stiffness only.

In the present research, all beams were subdivided into 24 brick elements as shown in Fig. 2(a). The placing of steel reinforcement in the mesh is illustrated in Fig. 2(b) for the specific case of the two high-ductility specimens HDCB3 and HDCB4.

4.3. Results

The analytical load-deflection characteristics for all the beams subjected to sequential loading are compared with the experimental behaviour in Figs. 3 to 7. In each instance, the total load is plotted against the deflections corresponding to the locations of the two concentrated loads, namely the middle of the main span (deflection D1) and the end of the overhang (deflection D2).

It can be seen that all analytical predictions of the peak load agree well with their experimental counterparts. Similarly, the maximum deflection at the main span is accurately estimated by the NLFEA. The maximum deflection of the overhang is also adequately mimicked by the analysis, although in some instances the numerical modelling may somewhat either underestimate (e.g. HDCB3, HDCB4) or overestimate (e.g., G21, G22) the ductility recorded experimentally: these effects are attributed to the discrepancies in stirrup spacing between experiments (actual spacing)

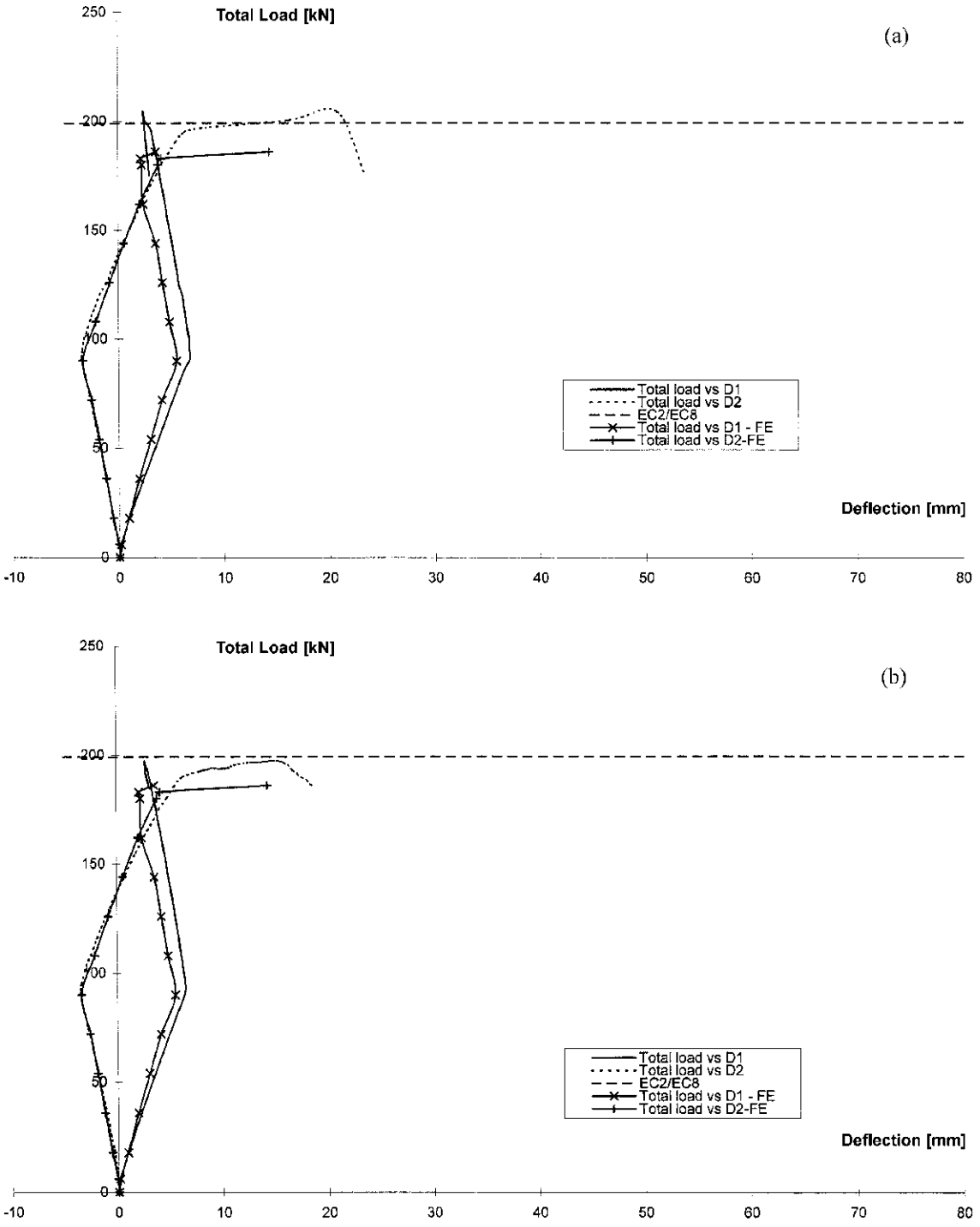

Fig. 3 Comparison of experimental and numerical load-deflection curves for specimens designed to EC2 and EC8 (high-ductility class): (a) beam HDCB3; (b) beam HDCB4

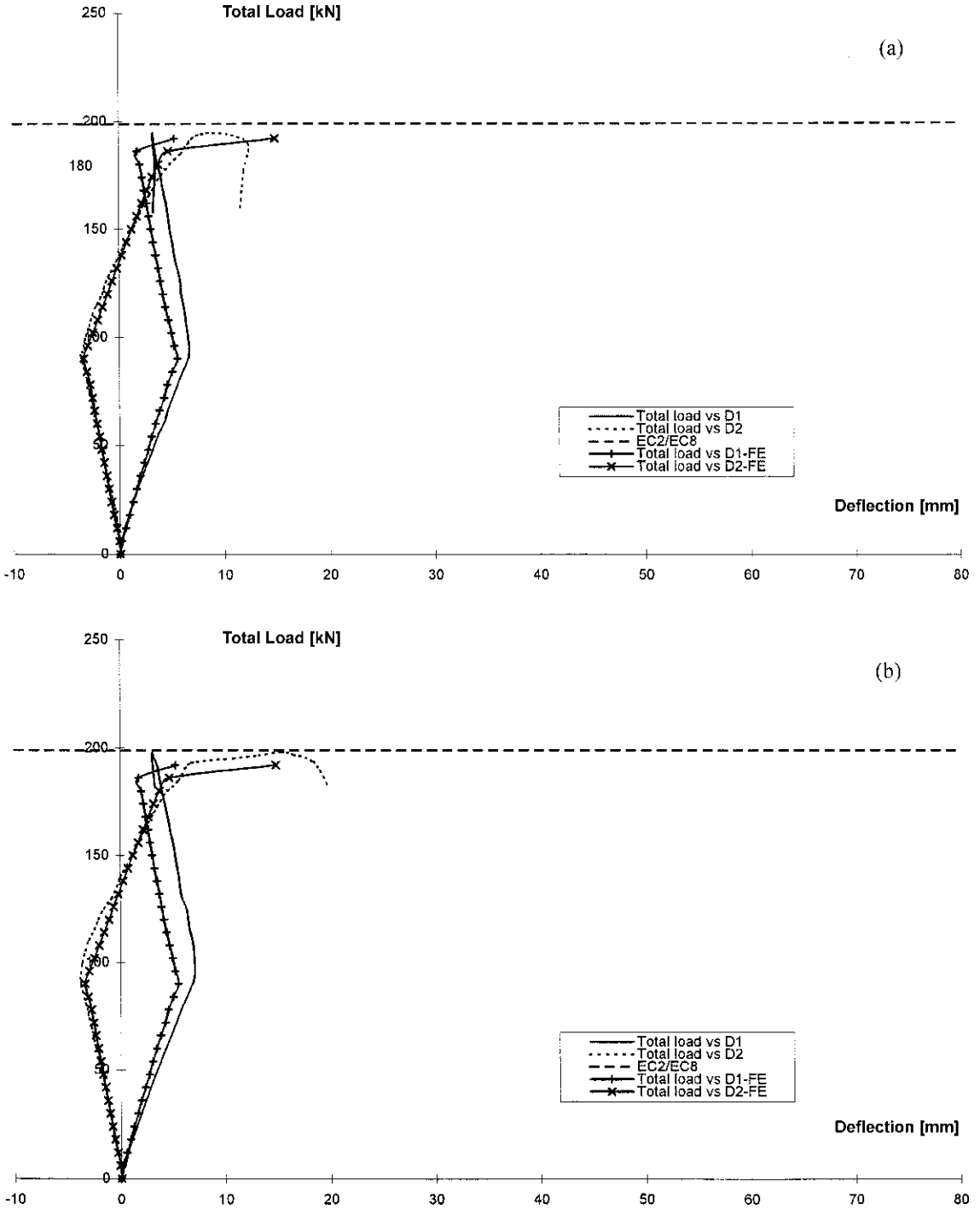

Fig. 4 Comparison of experimental and numerical load-deflection curves for specimens designed to EC2 and EC8 (medium-ductility class): (a) beam MDCB3; (b) beam MDCB4

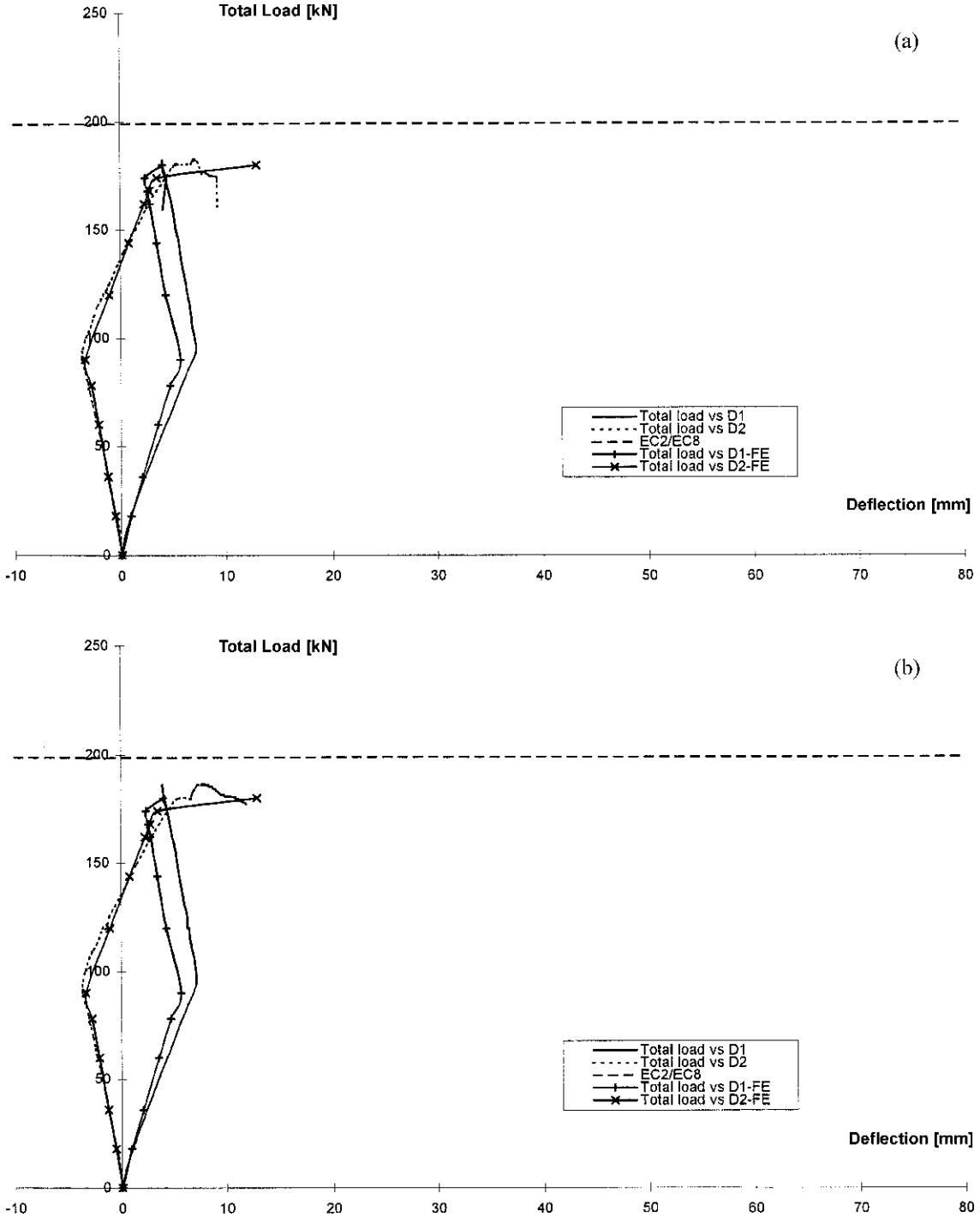

Fig. 5 Comparison of experimental and numerical load-deflection curves for specimens designed to EC2 and EC8 (low-ductility class): (a) beam LDCB3; (b) beam LDCB4

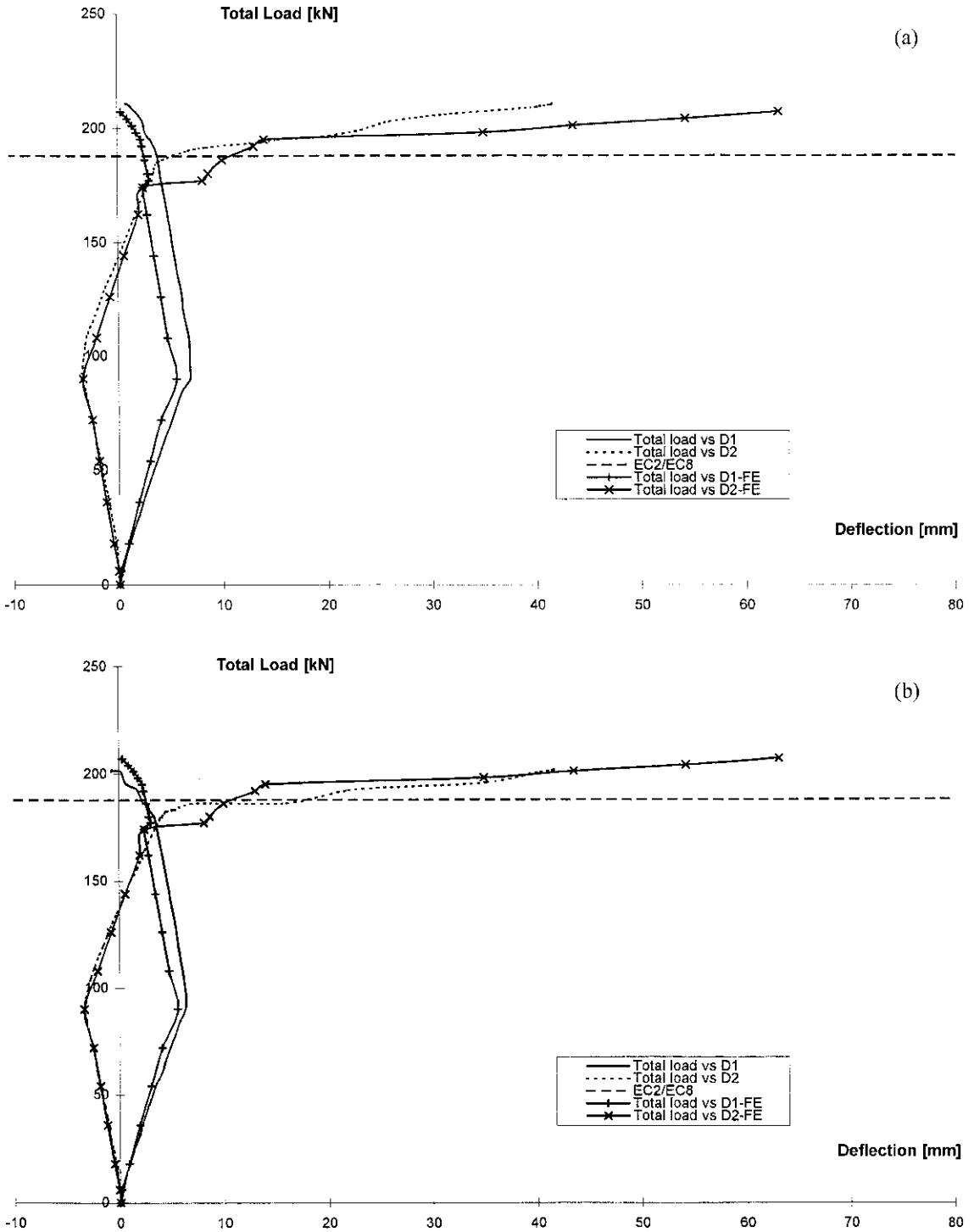

Fig. 6 Comparison of experimental and numerical load-deflection curves for specimens designed to GEC : (a) beam G21; (b) beam G22

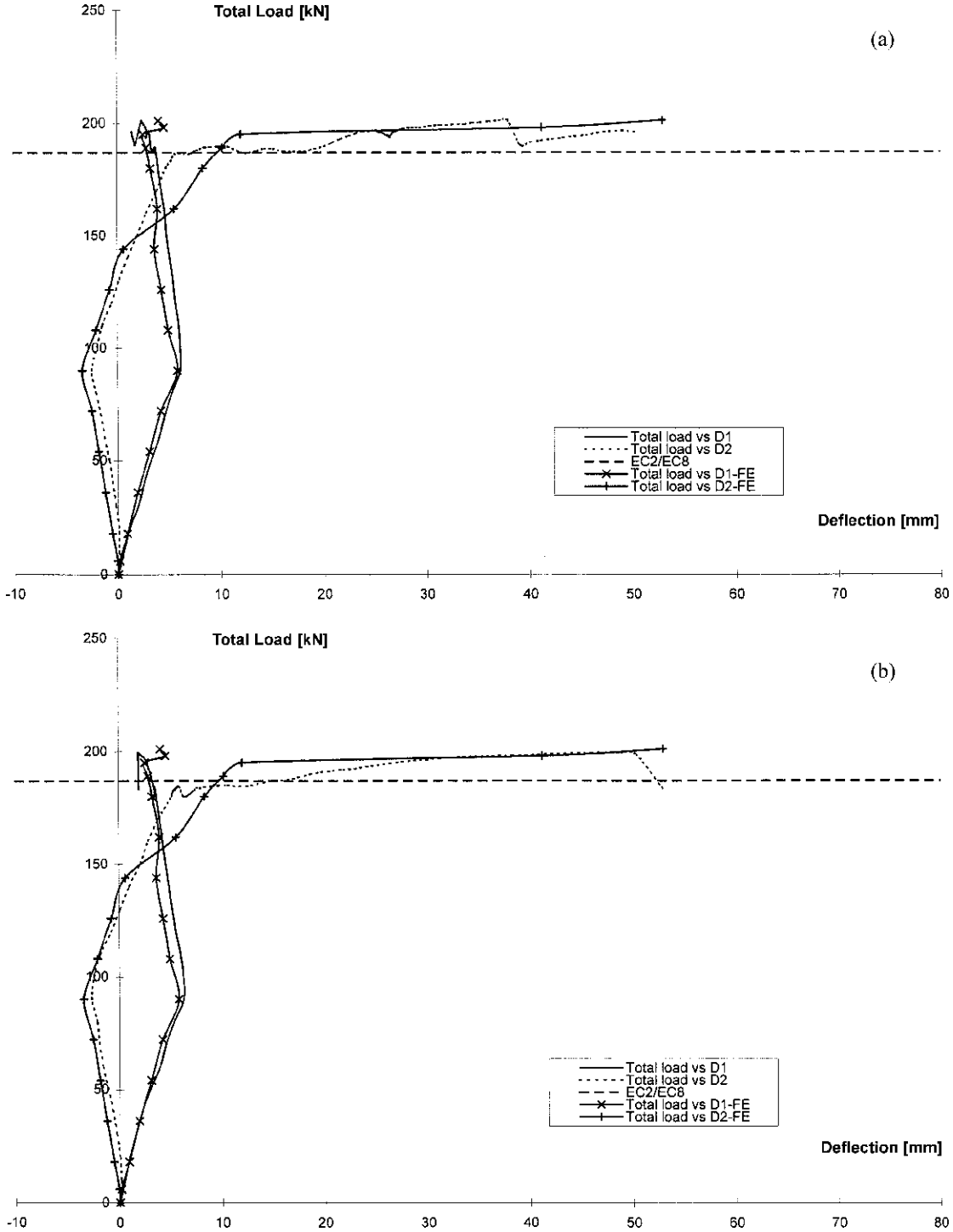

Fig. 7 Comparison of experimental and numerical load-deflection curves for specimens designed to the CFP method: (a) beam B1; (b) beam B2; (c) beam B3; (d) beam B4

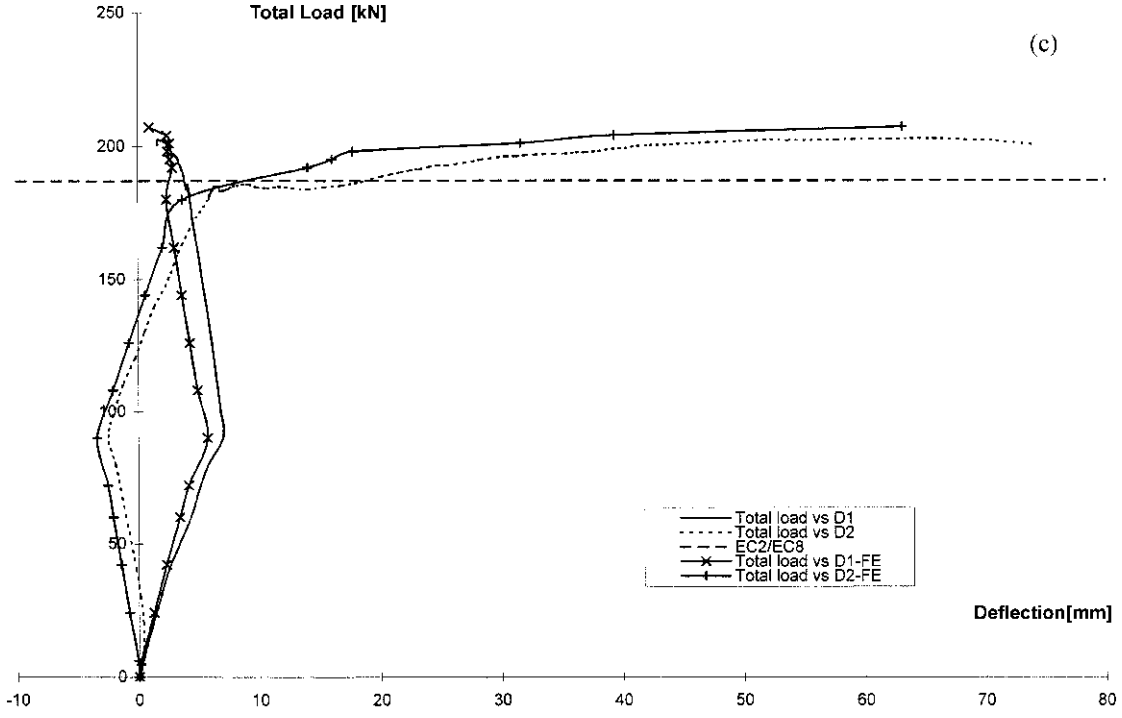

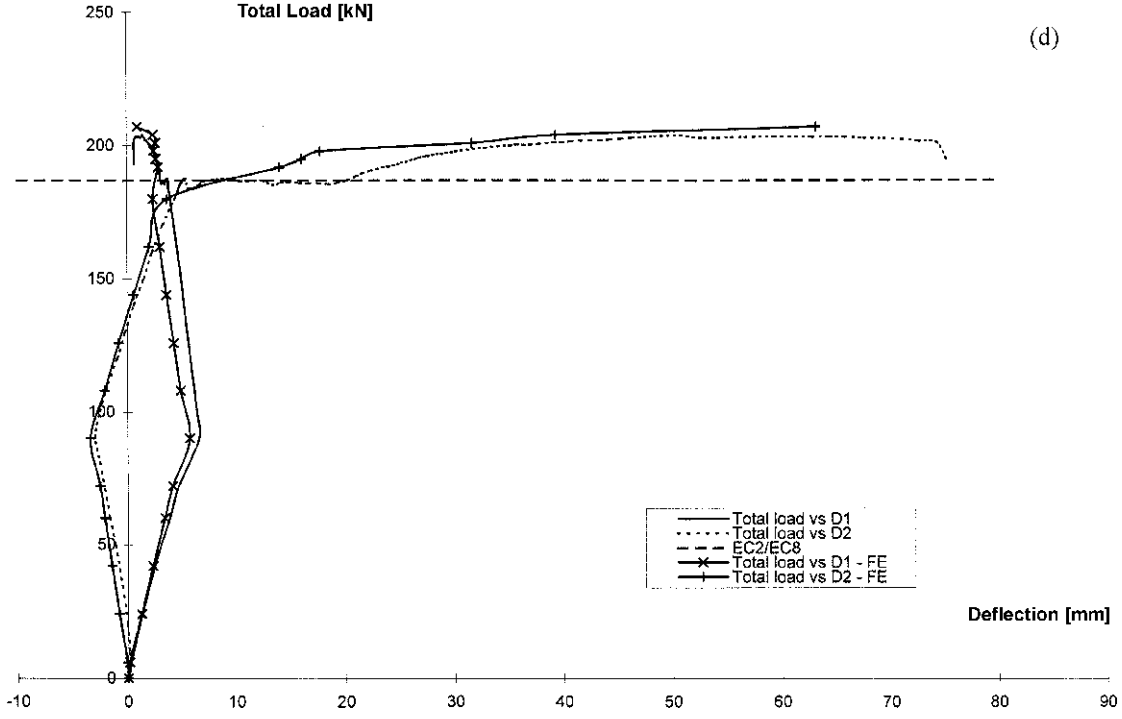

Fig. 7 Continued

and FE modelling (smeared spacing) and to the use of finite load steps. Such simple and economical analysis is conducted within an engineering - rather than a strictly "research" - context. Nevertheless, it is evident that the numerically predicted ductilities not only represent good estimates in all cases but also provide reliable pointers to the effect produced by the introduction of a given parameter (see, for example, the increase in ductility resulting from the addition of confinement reinforcement in the compression region of those beams designed to the CFP philosophy, i.e., compare B1, B2 with B3, B4).

5. Conclusions

The beams designed to EC2 and EC8 codes of practice were all supposed to have achieved their flexural capacity and required ductility. By varying the amount - and hence the spacing - of the transverse reinforcement, the only resulting difference should have been the deflection achieved, i.e., the ductility of the beams. However, in the case of sequential loading all beams but one (HDCB3) failed before their flexural capacities were reached. Moreover, all beams tested for sequential loading failed due to an inclined crack connecting the point load at the overhang with the support. The failure of the beams under sequential loading, therefore, appears to be due to the inability of the transverse reinforcement to control inclined cracking, even though the amount of shear reinforcement provided was sufficient to prevent brittle diagonal failure.

Members designed in accordance with EC2 and EC8 provisions had relatively poor ductility (when one considers that they were designed with ductility in mind). In fact, for sequential loading, all beams failed to exhibit the minimum ductility required by EC8, which recommends a minimum ductility factor of 3.5.

One conclusion from the tests on beams designed to EC2 and EC8 clauses, therefore, seems to be that - paradoxically, if one follows current code thinking - the transverse reinforcement actually caused the diagonal (although not brittle) failure of the beams before they reached their flexural capacity. This can be seen by reference to the members designed to the GEC: even though HDCB and MDCB specimens designed in accordance with EC2 and EC8 had more shear reinforcement (the total cross-sectional areas of transverse reinforcement were $3418\,mm^2$ for HDCB and $3217\,mm^2$ for MDCB) than the beams designed to the GEC ($2714\,mm^2$ of stirrups), the GEC members not only achieved (in all cases) their full flexural-capacity potential, but also exhibited consistently better ductility than the HDCB and MDCB specimens. However, the apparent safety of the Greek earthquake clauses in this particular study cannot always be guaranteed, as shown elsewhere (Kotsovos and Pavlović 1999, Jelić, *et al.* 2003).

Finally, Table 1 and Fig. 7 highlight the performance of the specimens designed in accordance to the proposed CFP method. The beams had considerably less transverse reinforcement, when compared to the beams which followed EC2/EC8 and GEC design guidelines, but still showed a superior performance, both in terms of strength and ductility. The beams designed to the CFP method had 60%, 55% and 30% less transverse reinforcement than the HDCB, MDCB and LDCB specimens respectively, and almost 50% less reinforcement than the beams designed to the GEC. All beams achieved their full flexural capacity, and much improved ductility when compared with the code-based members. Beams with additional confining transverse reinforcement in the compressive zone, tested under both proportional and sequential loading, failed in flexure with considerable ductility, a ductility which was much higher than that of the other beams tested in the current research programme. By confining the compressive zone at the location of the internal

supports, as stipulated by the CFP theory, the beams were able to sustain greater loads and improve further on ductility.

References

BS8110 (1985), Code of Practice for the Design and Construction of Concrete Structures.
EC2 (1991), European Code of Practice for the Design of Concrete Structures.
EC8 (1991), European Code for the Design of Earthquake Resistant Structures.
GEC (2000), Greek Earthquake Code.
Hitchings, D. (1980), *FINEL Programming Manual*, Imperial College, London.
Jelić, I. (2002), *Behaviour of Reinforced Concrete Beams: A Comparison between the CFP Method and Current Practice*, Ph.D. Thesis, University of London.
Jelić, I., Pavlović, M.N. and Kotsovos, M.D. (2003), "Towards the development of a method suitable for the strength assessment of existing reinforced concrete structures", *Proceedings of the FIB Symposium "Concrete Structures in Seismic Regions"*, Athens, May, Paper #246 (6 pages/on CD-ROM).
Kotsovos, M.D. (1982), "A fundamental explanation of the behaviour of reinforced concrete beams in flexure based on the properties of concrete under multiaxial stress", *Materials & Structures (RILEM)*, **15**, 529-537.
Kotsovos, M.D. (1983), "Effect of testing techniques on the post-ultimate behaviour of concrete in compression", *Materials & Structures (RILEM)*, **16**, 3-12.
Kotsovos, M.D. and Pavlović, M.N. (1995), *Structural Concrete: Finite-Element Analysis for Limit-State Design*, Thomas Telford, London.
Kotsovos, M.D. and Pavlović, M.N. (1999), *Ultimate Limit-State Design of Concrete Structures: A New Approach*, Thomas Telford, London.
Kotsovos, M.D. and Pavlović, M.N. (2001), "The 1999 Athens earthquake: causes of damage not predicted by structural concrete design methods", *The Structural Engineer*, **79**(15), 23-29.
Kotsovos, M.D. and Spiliopoulos, K.V. (1998a), "Modelling of crack closure for finite-element analysis of structural concrete", *Computers & Structures*, **69**, 383-398.
Kotsovos, M.D. and Spiliopoulos, K.V. (1998b), "Evaluation of structural-design concepts based on finite-element analysis", *Computational Mechanics*, **21**, 330-338.
Van Mier, J.G.M. (1986), "Multiaxial strain-softening of concrete: Part I. Fracture, Part II. Load-histories", *Materials & Structures (RILEM)*, **19**, 179-200.
Van Mier, J.G.M., Shah, S.P., Arnaud M., Balayssac, J.P., Bassoul, A., Choi, S., Dasenbrock, D., Ferrara, G., French, C., Gobbi, M.E., Karihaloo, B.L., Konig, G., Kotsovos, M.D., Labuz, J., Lange-Kornbak, D., Karkeset, G., Pavlović, M.N., Simsch, G., Thienel, K-C., Turatsinze, A., Ulmer, M., van Vliet, M.R.A. and Zissopoulos, D., (1997), *Materials & Structures (RILEM)*, **30**, 195-209.
Zienkiewicz, O.C. (1977), *The Finite-Element Method*, McGraw-Hill, London.